Structural Engineering and Mechanics, *Vol. 47, No. 2 (2013) 265-286*
DOI: http://dx.doi.org/10.12989/sem.2013.47.2.265

Study on economic performances of multi-span suspension bridges part 1: simple estimation formulas

Li-wen Zhang*[1], Ru-cheng Xiao[1], Bin Sun[1], Yang Jiang[1], Xue-yi Zhang[1], Dong-li Zhuang[2], Yun-gang Zhou[2] and Xue Tu[3]

[1]Department of Bridge Engineering, Tongji University, 1239 Siping Rd., Shanghai 200092, China
[2]Architectural Design & Research Institute of Tongji University (Group) Co., Ltd., Shanghai 200092, China
[3]LIN Tung-yan & LI Guo-hao Consultants LTD., Shanghai 200092, China

(Received January 13, 2013, Revised July 15, 2013, Accepted July 17, 2013)

Abstract. A study on economic performances of consecutive multi-span suspension bridges is carried out. In this part of the study, material amount and structural cost estimation formulas of the bridges is derived based on the structural ultimate carrying capacity. The bridge cost includes the part of superstructure and the part of substructure. Three types of bridge foundations, bored piles, concrete caissons and floating foundations, are considered in substructure. These formulas are to be used for the parametric study of the bridge cost in order to define its more economical layout under different conditions in the part two of the study.

Keywords: multi-span suspension bridge; economic performance; economical layout; cost estimation formula

1. Introduction

The construction of bridges crossing straits has been favored by authorities for reducing higher traffic pressures of air transports and navigations caused by global businesses and communications increasing for recent years. At last 4 projects have been completed since 1990s: Great Belt Bridges (Danish) in 1998, Oresund Link (Danish) in 2000, Hangzhou Bay Bridges (China) in 2008 and Qingdao Bay Bridges (China) in 2011. Besides, some larger projects are to be constructed in Fehmarn Belt, Taiwan Strait, Qiongzhou Strait and Gibraltar strait, etc., in the near future (Ge and Xiang 2006, 2008a, b, 2011, Gimsing 2009). In these projects, consecutive multi-span suspension bridge is recognized as a valid alternative to the ultra-long span length bridges only having one main span, e.g., typical suspension bridges and cable-stayed bridges, or these bridges in series (Starossek 1996, Virlogeux 1999, Buckland and Matson 2006, Clemente *et al*. 2000, Kitagawa *et al*. 2001, Svensson 2007, Tang 2007, Sun *et al*. 2010, Yoshimura and Kawahara 2010, Zhang *et al*. 2011a, b, Zhang and Xiao 2011c).

There are some studies focusing on multi-span suspension bridges to be conducted for many years, such as: the deflection theory of multi-span suspension bridges considering the deflection of

∗Corresponding author, Ph.D., E-mail: unitstate@gmail.com

http://www.techno-press.org/?journal=sem&subpage=8 ISSN: 1225-4568 (Print), 1598-6217 (Online)

towers (Sato 1971); the analytical method used to calculate the structural natural frequency and the mode shape as well as the dynamic response (Hayashikawa and Watanabe 1982); the static stability (Nazir 1986); the analysis of multi-span suspension bridges with very long span up to 2000m (Fosberp 2001, Yoshida *et al*. 2004); the analysis for double main bridges constructed or at design stage such as the Jiangsu Taizhou Bridge over Yangtze River with double main-span of 2×1080m completed in 2012, the Anhui Maanshan Bridge over Yangze River in China and the New Millennium Grand Bridge in Korea (Choi *et al*. 2010, Daniel *et al*. 2010, Forsberg 2001, Ge and Xiang 2006, 2008a, b, 2011, Jung *et al*. 2010, Luo *et al*. 2011); the aerodynamic flutter analysis of a new suspension bridge with double main spans (Zhang *et al*. 2011); and the simple analytical formulas calculating suspension bridges with double main cables in the vertical plan (Zhang *et al*. 2012), etc. Besides, the simple analytical formulas and parametric analysis for multi-span suspension bridges have been developed and completed in other studies of the author for investigating its mechanical performance.

Another key factor constructing a multi-span suspension bridge to cross a strait, however, is how to define a reasonable layout for obtaining the best economic performance besides the best mechanical performance. This is because that the quantities of strait crossing constructions are very huge. Unfortunately, there are few studies focusing on it expect for the work only to assess material requirements of superstructure of traditional cable-stayed bridges and suspension bridges by Gimsing (2012) and Lewis (2012). Thus, some researches about the economic performance of multi-span suspension bridges are carried out in this study. In this part, the estimation formulas of the bridge cost and material amount are derived based on the structural ultimate carrying capacity. The bridge cost includes two parts: one part of superstructure and the other part of substructure. Three types of bridge foundations, bored piles, concrete caissons and floating foundation, are considered in substructure.

2. Superstructure cost

2.1 Assumption and decomposition of bridge

The fundamental approach for the study is as follows:

- Only the self-weight and a uniformly distributed live load are taken into account in the calculation of the axial force.
- The material amount of each part is decided by the setting of the stress equaling the material strength.
- The possible bending moment is taken into account in the material strength.
- And the calculation of structural force does not consider the structural seconder order effects.

A multi-span consecutive suspension bridge could be divided into five parts: suspension systems consisting of main cables and suspenders, girders, towers, anchorages and foundations. The four formers are superstructure, and the last one is substructure.

The composition of multi-span suspension bridges is similar as typical suspension bridges except for the tower compositions: the tower system consists of main-span towers and side-span towers in multi-span suspension bridges but only consists of two side-span towers in typical suspension bridges. Figs. 1(a)-(c) offer the compositions of a multi-span suspension bridge having more than two main spans, a multi-span suspension bridge having two main spans and a typical suspension bridge, respectively.

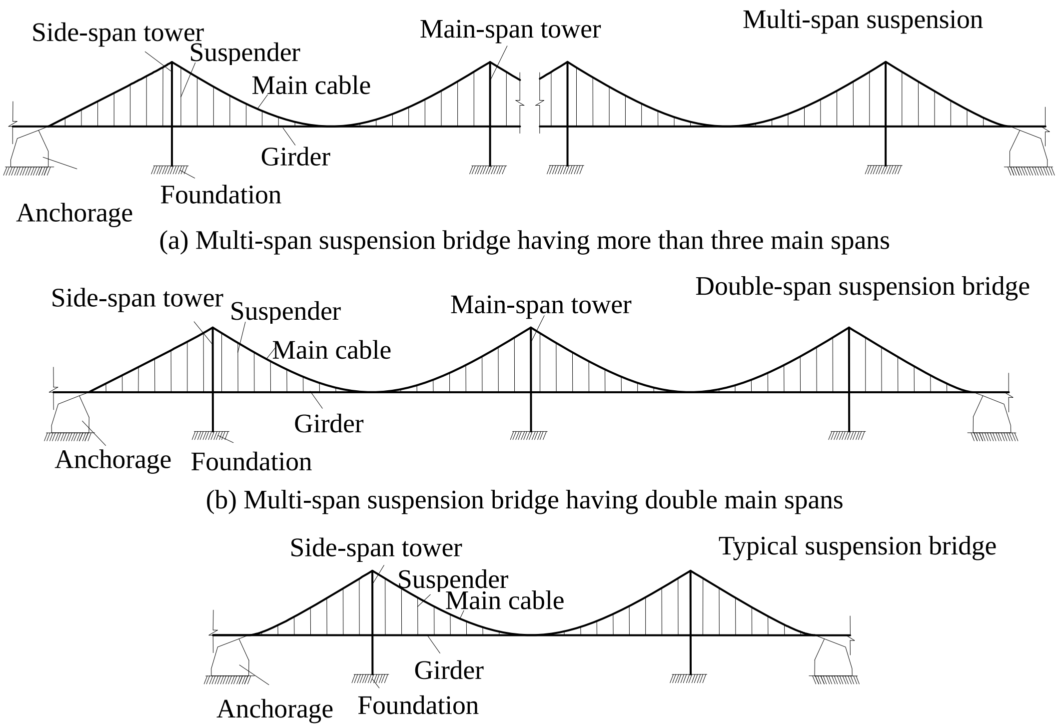

(a) Multi-span suspension bridge having more than three main spans

(b) Multi-span suspension bridge having double main spans

(c) Typical suspension bridge

Fig. 1 Compositions of suspension bridges

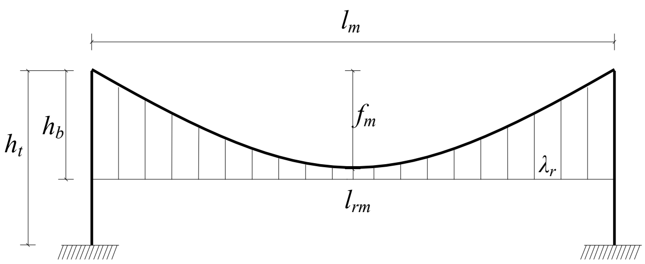

Fig. 2 Suspension system

The cost of a suspension bridge could be expressed as follows

$$C = C_{sus} + C_{tow} + C_{arc} + C_{base} + C_{gir} \tag{1}$$

where C is the cost of a suspension bridge; C_{sus} is the cost of suspension systems; C_{tow} is the cost of towers; C_{arc} is the cost of anchorages; C_{base} is the cost of foundations; and C_{gir} is the cost of girders.

2.2 Bridge suspension system

The cost of the suspension system at one main span is simplified as Fig. 2 where l_m is the span

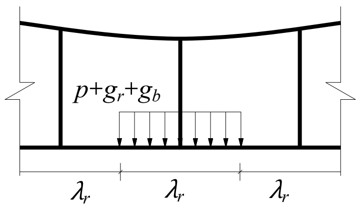

Fig. 3 Sketch of suspender carrying load

length, f_m is the cable sag, l_{rm} is the mid-span suspender length, λ_r is the distance between two adjacent suspenders, h_t is the tower height, and h_b is the tower height above the pavement.

Two subjects need to be calculated in this system: the one is the material consumption of the suspenders, the other one is the material consumption of the main cable. As for a suspender, it carries the live load p, the girder weight g_b and the uniformly distributed suspender weight g_r in the region of λ_r, just as shown in Fig. 3. If the tensile strength and crossing-section area of the suspender is σ_r and A_r respectively, a mechanical balance in the suspender crossing-section can be established by Eq. (2).

$$\sigma_r A_r = \left(g_r + g_b + p\right)\lambda_r \tag{2}$$

The material consumption of the suspender is obtained based on Eq. (2), which is expressed as

$$q_{rm} = A_r l_r \gamma_r = \frac{\left(g_r + g_b + p\right)\lambda_r}{\sigma_r} l_r \gamma_r \tag{3}$$

where q_{rm} is the material consumption of the suspender, l_r is the suspender length and γ_r is the suspender unit weight.

The material consumption of the suspenders at this span is calculated by summing up the material consumption of each suspender calculated by Eq. (3), which is expressed in Eq. (4).

$$Q_{rm} = \sum_{r=1}^{n} q_{rm} = \sum_{r=1}^{n} A_r l_r \gamma_r = \sum_{r=1}^{n} \frac{\left(g_r + g_b + p\right)\lambda_r}{\sigma_r} \gamma_r l_r \tag{4}$$

where n is the number of the suspenders at this span.

However, it is a complex and troublesome task to calculate Q_{rm} by Eq. (4) because that the number of the suspenders and the length of each suspender need to be calculated. Therefore, the discrete distributed suspenders are equivalent to a continuous suspender membrane (Gimsing 2012), and Eq. (4) is converted to a continuous integral expressed in Eq. (5).

$$Q_{rm} = 2\int_0^{\frac{l_m}{2}} \frac{\left(g_r + g_b + p\right)}{\sigma_r} \gamma_r l_r \mathrm{d}x \tag{5}$$

where l_r is the suspender membrane length that is a function related to the cable profile and the suspender position. By assuming a parabola profile of the cable, l_r is expressed as

$$l_r = l_{rm} + \frac{4f_m}{l_m^2} x^2 \tag{6}$$

By substituting Eq. (6) into Eq. (5), the material consumption of the suspenders in the main span is obtained, as follows

$$Q_{rm} = \gamma_r \left(g_b + p + g_r\right)\left(l_{rm} + \frac{f_m}{3}\right) l_m \Big/ \sigma_r \tag{7}$$

The uniformly distributed suspender weight g_r needs to be calculated for solving Eq. (7). Assuming the average length of the suspenders is l_{ra}, the uniformly distributed suspender weight g_r is expressed as Eq. (8).

$$\begin{cases} g_r = A_r \gamma_r l_{ra} / \lambda_r \\ l_{ra} = \dfrac{f_m}{3} + l_{rm} \end{cases} \tag{8}$$

Substituting Eq. (8) into Eq. (2), the crossing section and the uniformly distributed weight of the suspenders is obtained, just as shown in Eq. (9).

$$\begin{cases} g_r = \dfrac{\gamma_r}{\sigma_r - \left(\dfrac{1}{3} f_m + l_{rm}\right)\gamma_r}\left(g_b + p\right)\left(\dfrac{1}{3} f_m + l_{rm}\right) \\ A_r = \dfrac{\lambda_r}{\sigma_r - \left(\dfrac{1}{3} f_m + l_{rm}\right)\gamma_r}\left(g_b + p\right) \end{cases} \tag{9}$$

The crossing section area of the main span cable also can be calculated based on the mechanical balance expressed in Eq. (10), which is shown in Eq. (11).

$$H_m = \frac{\left(p + g_r + g_b + A_{mc}\gamma_c\right) l_m^2}{8 f_m} \tag{10}$$

where H_m and A_{mc} is the horizontal force and the cross section area of the main-span cable respectively; σ_c is the cable tensile strength; and γ_c is the cable volume weight.

Besides Eq. (10), H_m also equals $T_{\max} \cdot \cos\alpha_{\max}$. $T_{\max}$ and $\alpha_{\max}$ is the cable's force and dip angle at the tower top respectively. $T_{\max}$ could be recognized as $A_{mc} \cdot \sigma_c$, and $\alpha_{\max}$ equals arctan ($4f_m/l_m$). By taking $H_m = T_{\max} \cdot \cos\alpha_{\max}$ into Eq. (10), A_{mc} is obtained as follows

$$A_{mc} = \frac{\left(g_b + p + g_r\right) l_m \sqrt{l_m^2 + 16 f_m^2}}{8\sigma_c f_m - \gamma_c l_m \sqrt{l_m^2 + 16 f_m^2}} \tag{11}$$

The material consumption of the main-span cable is obtained by multiplying its cross section area, curve length and volume weight, as follows

$$Q_{mc} = A_{mc} \gamma_c S_{mc} \tag{12}$$

where S_{mc} is the curve length of the main-span cable expressed in Eq. (13).

$$S_{mc}=\frac{l_m}{2}\left\{\left[1+16\left(\frac{f_m}{l_m}\right)^2\right]^{\frac{1}{2}}+\frac{\ln\left[\frac{4f_m}{l_m}+\left[1+16\left(\frac{f_m}{l_m}\right)^2\right]^{\frac{1}{2}}\right]}{\frac{4f_m}{l_m}}\right\} \tag{13}$$

As for the material consumption of side-span suspenders and side-span cables, it is still calculated by this method. A side-span suspender length is expressed in Eq. (14)

$$\begin{cases} l_r=4f_a\left(\dfrac{x}{l_s}\right)^2+\dfrac{\left(h_b-4f_a\right)}{l_s}x \\ f_a=\left(\dfrac{l_s}{l_m}\right)^2 f_m \end{cases} \tag{14}$$

where f_a is the side-span cable sag; l_s is the side span length; x is the distance from the suspender to the anchor point of the side-span cable; and h_b is the tower height above the pavement. The material consumption of side-span suspenders is

$$\begin{cases} Q_{rs}=2\displaystyle\int_0^{l_s}\frac{\left(g_{sr}+g_b+p\right)}{\sigma_r}\gamma_r l_r \mathrm{d}x=\frac{\left(g_{sr}+g_b+p\right)}{\sigma_r}\gamma_r\left(h_b l_s-\frac{4}{3}f_a l_s\right) \\ g_{sr}=\left(\dfrac{h_b}{2}-\dfrac{2}{3}f_a\right)\left(g_b+p\right)\gamma_r\Big/\left[\sigma_r-\left(\dfrac{h_b}{2}-\dfrac{2}{3}f_a\right)\gamma_r\right] \end{cases} \tag{15}$$

where Q_{sr} is the material consumption of side-span suspenders, g_{sr} is the unit weight of side-span suspenders, and l_s is a side span length.

The material consumption of side-span main cables is expressed in Eq. (16)

$$\begin{cases} Q_{sc}=2\gamma_c A_{mc} S_{sc} \\ S_{sc}=\dfrac{l}{4n_s}\left\{a\sqrt{a^2+1}-b\sqrt{b^2+1}+\ln\dfrac{a+\sqrt{a^2+1}}{b+\sqrt{b^2+1}}\right\} \\ n_s=4f_a/l_s,\ a=\left(h_b+4f_a\right)/l_s,\ b=\left(h_b-4f_a\right)/l_s \end{cases} \tag{16}$$

where Q_{sc} is the material consumption of side-span main cables and S_{sc} is the curve length of the cable at a side span.

Assuming the unit cost of suspenders and main cables is μ_c and μ_r respectively, and the cost of suspension systems could be obtained

$$C_{sus}=n_{mc}\mu_c Q_{mc}+n_{mc}\mu_r Q_{rm}+\mu_c Q_{sc}+\mu_r Q_{rs} \tag{17}$$

where n_{mc} is the number of main spans.

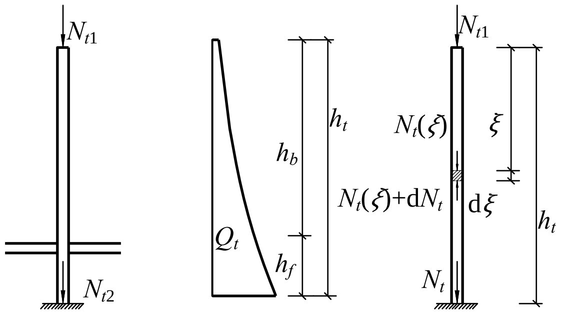

Fig. 4 Loading state of bridge tower

2.3 Bridge tower and girder

Fig. 4 offers the loading state of a bridge tower, in which N_{t1} and N_{t2} is the compression on the tower top and bottom respectively, h_f is the tower height below the pavement, ξ is the distance from the pylon top to the calculated section, $N_t(\xi)$ is the compression on the calculated section, and Q_t is the material consumption of the tower.

A mechanical balance equation is established based on Fig. 4, as follows

$$\begin{cases} N_t(\xi)+A_t(\xi)\gamma_t \mathrm{d}\xi = N_t(\xi)+\mathrm{d}N_t(\xi) \\ A_t(\xi) = N_t(\xi)/\sigma_t \end{cases} \tag{18}$$

where $A_t(\xi)$ is the cross section area of the calculated section and γ_t is the tower volume weight. The compression on the calculated section $N_t(\xi)$ can be obtain by solving Eq. (18), which is expressed in Eq. (19).

$$N_t(\xi) = N_{t1}\exp\left(\frac{\gamma_t}{\sigma_t}\xi\right) \tag{19}$$

where σ_t is the compressive strength of the tower. The cross section area $A_t(\xi)$ is obtained by substituting Eq. (19) into Eq. (18). The material consumption of the tower is computed by integrating $A_t(\xi)$ within the tower height, which is expressed in Eq. (20).

$$Q_t = \int_0^{h_t} N_t(\xi)\frac{\gamma_t}{\sigma_t}\mathrm{d}\xi = N_{t1}\left\{\exp\left[\frac{\gamma_t}{\sigma_t}h_t\right]-1\right\} \tag{20}$$

As for a main-span tower, N_{t1} is two times as the vertical component of a main-span cable force, which is expressed in Eq. (21). But as for a side-span tower, N_{t1} is the sum of a side-span cable force vertical component and a main-span cable force vertical component, which is expressed in Eq. (22).

$$N_{t1} = 8\frac{H_m f_m}{l_m} \tag{21}$$

$$N_{t1} = H_m\left(\frac{4f_m}{l_m} + \frac{h_b + 4f_a}{l_s}\right) \tag{22}$$

The material consumption of a main-span tower and a side-span tower could be obtained by substituting Eqs. (21) and (22) into Eq. (20), respectively, as follows

$$\begin{cases} Q_{mt} = 8\dfrac{H_m f_m}{l_m}\left\{\exp\left[\dfrac{\gamma_t}{\sigma_t}h_t\right] - 1\right\} \\ Q_{st} = H_m\left(\dfrac{4f_m}{l_m} + \dfrac{h_b + 4f_a}{l_s}\right)\left\{\exp\left[\dfrac{\gamma_t}{\sigma_t}h_t\right] - 1\right\} \end{cases} \tag{23}$$

where Q_{mt} and Q_{st} is the material consumption of the main-span tower and the side-span tower, respectively.

Then, the cost of suspension bridge towers is obtained, being shown in Eq. (24).

$$C_{tow} = 2\mu_t Q_{st} + (n_{mc} - 1)\mu_t Q_{mt} \tag{24}$$

where μ_t is the unit cost of the towers.

The material consumption of bridge girders is the product of the length and the unit weight of the girders, just as shown in Eq. (25)

$$Q_{gir} = Lg_b \tag{25}$$

where Q_{gir} is the material consumption of bridge girders, and L is the length of the girders.

The cost of girders is expressed as follows

$$C_{gir} = \mu_g Q_{gir} \tag{26}$$

where μ_g is the unit cost of the girders.

2.4 Bridge anchorage

Anchorage, which is shown in Fig. 5(a), is used to balance the cable force in suspension bridges. The equation of the relationship between an anchorage material consumption and cable forces could be established according to the rules regarding anti-slide stability in Chinese code of JTG D63-2007.

$$\frac{(Q_{sa} - V_{sc})\mu_{arc}}{H_m} = 2 \tag{27}$$

where V_{sc} is the vertical component of the cable force at a side span, Q_{sa} is the material consumption of an anchorage, and μ_{arc} is the friction coefficient between the anchorage and the ground. Q_{sa} is expressed as

$$Q_{sa} = 2H_m / \mu_{arc} + V_{sc} \tag{28}$$

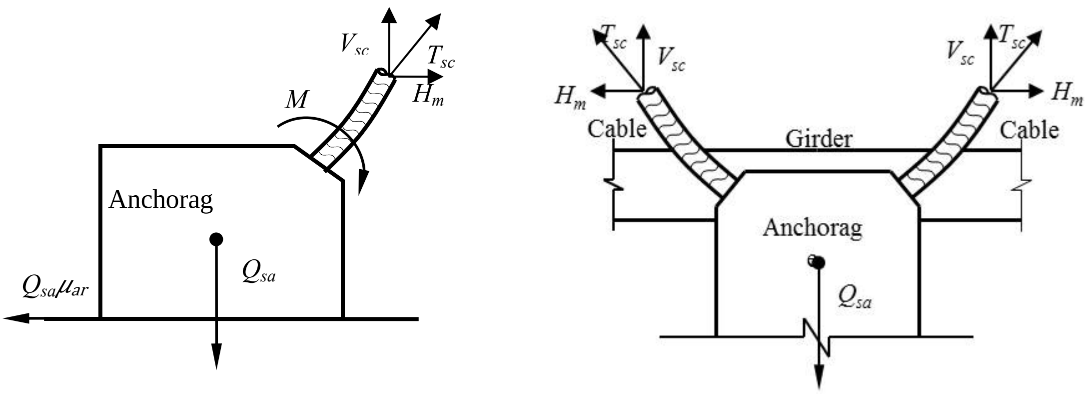

(a) (b)

Fig. 5 Anchorage (a) General anchorage (b) Shared anchorage over water

$$\begin{cases} V_{sc} = H_m \tan\alpha \\ \tan\alpha = \left(h_b + 4f_a\right)/l_s \end{cases} \tag{29}$$

After taking Eq. (29) into Eq. (28), Q_{sa} could be obtained

$$Q_{sa} = H_m \left(2/\mu_{arc} + \tan\alpha\right) \tag{30}$$

However, there is another anchorage generally built in water, called "shared anchorage", which is shared by two adjacent typical suspension bridges in the case of several typical suspension bridges connected in series. As for a shared anchorage, it could be simplified to a composition consisting of two parts: the part above water, and the part below water. The part above water carries the cable force from the side-span cable of two adjacent suspension bridges, just as shown in Fig. 5(b).

The material consumption of this part could be obtained according the method of calculating Q_{sa}, but in which H_m and V_{sc} is replaced by the horizontal component of a side-span cable force induced by live load and replaced by two times vertical component of a side-span cable force induced by total load respectively. It is because that the dead load-induced force of cables at two adjacent side spans have been balanced each other in the horizontal direction. The material consumption of this part is expressed as

$$\begin{cases} Q_{ma1} = 2\left(\dfrac{H_p}{\mu_{arc}} + V_{sc}\right) \\ V_{sc} = H_m \tan\alpha, H_p = \dfrac{pl_m^2}{8f_m} \end{cases} \tag{31}$$

where Q_{ma1} is the material consumption of the part above water.

For the part of the anchorage below water, it supports the anchorage above-water and carries the weight of itself as the bridge foundation in the form of a concrete caisson generally. That shows the loading condition as similar as the bridge tower, which c0ould be simplified as Fig. 6.

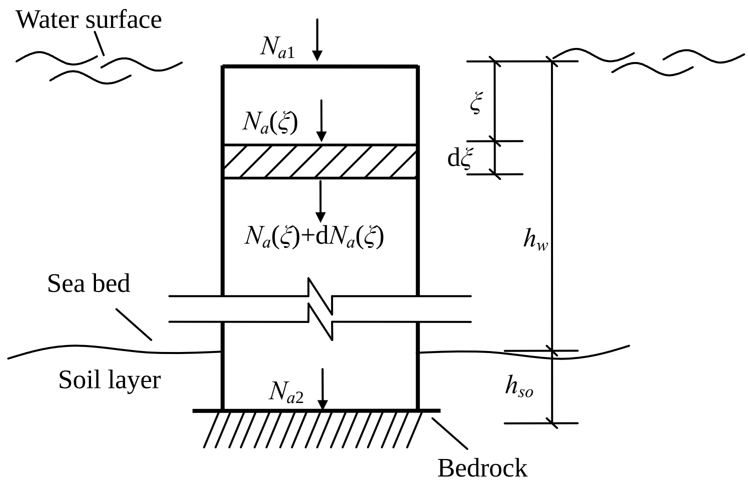

Fig. 6 Loading condition of shared anchorage below-water part

The material consumption of this part Q_{ma2} could be obtained by referring to Eq. (20). But, it is noted that the minimum area of the part top, A_{a1}, is decided by N_{a1}/σ_{a1}, and it makes the compression, $N_a(\xi)$, not necessarily equal the product of the section area and the material strength when to calculate the compression by Eqs. (18) and (19) in the part. Thus, an assumption of $A_{ai}(\xi)=A_{Nai}(\xi)-(A_N-A_{a1})$ is proposed, in which $A_{Nai}(\xi)$, equaling $A_N \cdot \exp(\gamma_{a2} x/\sigma_{a2})$, is the section area to meet the compression $N_a(\xi)$; A_N, equaling N_{a1}/σ_{a2}, is the section area of the part top to meet the compression N_{a1}.

After taking $N_a(\xi)$ calculated by the assumption into Eq. (20), the material amount of the part is obtained, just as shown in Eq. (32).

$$Q_{ma2} = N_{a1}\left\{\exp\left[\frac{\gamma_{a2}}{\sigma_{a2}}\left(h_w + h_{so}\right)\right]-1\right\} + \frac{N_{a1}}{\sigma_{a1}}\gamma_{a2}\left(h_w + h_{so}\right) - \frac{N_{a1}}{\sigma_{a2}}\gamma_{a2}\left(h_w + h_{so}\right) \tag{32}$$

where N_{a1} is the compression from the above-water part, equaling Q_{ma1}; γ_{a2} is the caisson volume weight; σ_{a1} is the compressive strength of the anchorage above water; σ_{a2} is the compressive strength of the caisson; h_w is water depth; and h_{so} is the thickness of soil layer. The floatage of water and the frictional resistance of soil for the caisson are not considered for simplicity in this calculation.

Then, the cost of the shared anchorage could be obtained by adding up the cost of the two parts, just as shown in Eq. (33).

$$C_{ma} = C_{ma1} + C_{ma2} = \mu_{ma1} Q_{ma1} + \mu_{ma2} Q_{ma2} \tag{33}$$

where C_{ma} is the cost of the shared anchorage, μ_{ma1} is the unit cost of constructing the part above water, and μ_{ma2} is the unit cost of constructing the part below water.

The cost of bridge anchorages could be expressed as:

$$C_{arc} = 2\mu_{sa} Q_{sa} + \left(n_{mc} - 1\right) C_{ma} \tag{34}$$

where μ_{sa} is the unit cost of the side-span anchorages.

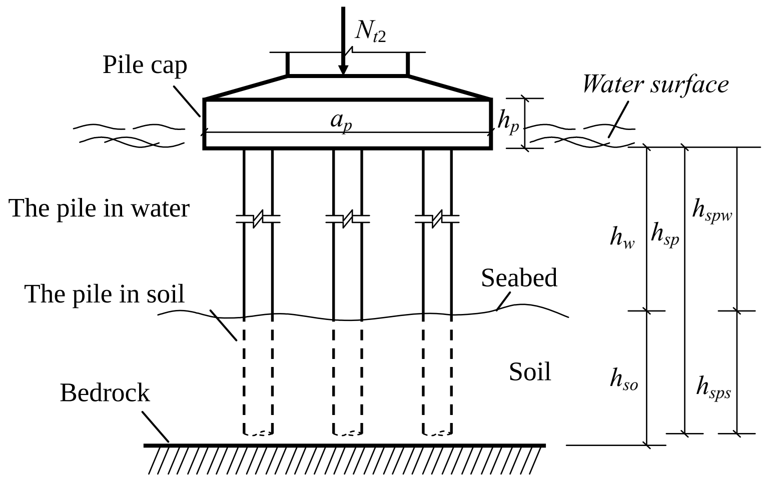

Fig. 7 Sketch of the bored pile

3. Substructure cost

The material consumption calculation of substructure cost is so difficult, not only because of various foundation types, but also because of various seabed geological conditions. Thus, a simplified geological condition consisting of soil and bedrock is applied, just as shown in Fig. 6. The soil is assumed to be composed of single soil stratum having the side friction=q_{sk} and the bearing capacity =q_{sr}, and the bedrock is assumed to have enough compressive strength to resist the compression from bridge foundations. Besides, three foundations are selected as the design of substructure. These foundations are bored pile, concrete caisson, and floating system called "floating foundation" which consists of floating box, cable and suction anchor.

3.1 Bored piles

It generally consists of three parts: the pile cap, the pile in water and the pile in soil. Fig. 7 offers the sketch of a bored pile, in which N_{t2} is the compression from bridge superstructure, a_p and h_p is the width and thickness of the pile cap, h_{spw} and h_{sps} is the length of the pile in water and in soil respectively, h_{sp} is the total length of the pile, h_w is water depth, and h_{so} is the thickness of soil.

Actually, it is so difficult to define the size of the pile cap accurately not only for its loading status but also for the need of the defining structural requirement by code. Thus, there is an assumption proposed for simplicity that the section area and the thickness of the pile cap is proportion to the contact area between the pile cap and the tower , just as shown in Eq. (35)

$$\begin{cases} A_{bp} = C_{bpa} A_{t2} \\ h_p = C_{bph} A_{t2} \end{cases} \tag{35}$$

where A_{bp} is the section area of the pile cap; A_{t2} is the contact area between the pile cap and the tower; C_{bpa} and C_{bph} is the coefficient of the pile cap section area and thickness respectively, which could be estimated according to engineering cases. Sutong Bridge is referred, in which C_{bpa} is about 11 and C_{bph} is about 0.8.

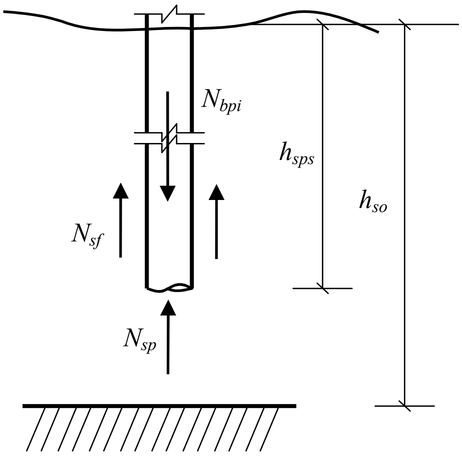

Fig. 8 Force acting on the pile in soil

By assuming a cube shaped pile cap, the material consumption of the pile cap is expressed as follows

$$Q_{bp} = A_{bp}h_p = C_{bpa}C_{bph}\gamma_{bp}A_{t2}^2 \tag{36}$$

where Q_{bp} is the material consumption of the pile cap; and γ_{bp} is the volume-weight of the pile cap.

A_{t2} is defined generally according to the force from the tower for simplicity, which is expressed as

$$A_{t2} = N_{t2}/\sigma_t \tag{37}$$

A pile having 2.8m diameter is applied referring to Sutong Bridge. Thus, the number of piles in the bored pile is obtained as shown in Eq. (38)

$$n_{bp} = \frac{N_{t2} + Q_{bp}}{A_{bpi}\sigma_{bpi}} \tag{38}$$

where σ_{bpi} is the compressive strength of piles; and A_{bpi} is the section area of the pile, which equals $1.96\pi\text{m}^2$.

The length of a bored pile is composed of two parts: one equaling water depth is the part in water; another is the part in soil. Fig. 8 describes the forces acting on the pile in soil, in which N_{bpi} is the combination of the pile weight and the force from the pile cap, N_{sf} is the side friction of soil along the pile shaft, and N_{sp} is the end bearing of the pile.

Based on the mechanical balance, Eq. (39) is established

$$N_{bpi} = N_{sf} + N_{sp} \tag{39}$$

where N_{bpi}, N_{sf} and N_{sp} is calculated by the equation as follows

$$\begin{cases} N_{bpi} = A_{bpi}\sigma_{bpi} + A_{bpi}\gamma_{bpi}h_{sp}, h_{sp} = h_{spw} + h_{sps} \\ N_{sf} = D_{spi}\pi q_{sk}h_{sps}, N_{sp} = A_{bpi}q_{sr} \end{cases} \tag{40}$$

where D_{spi} is the diameter of the pile. The length of the pile in soil could be calculated based on Eq. (39) and Eq. (40), which is expressed in Eq. (41).

$$h_{sps} = \frac{A_{bpi}\left(\sigma_{bpi} + \gamma_{bpi} h_{spw} - q_{sr}\right)}{D_{bpi}\pi q_{sk} - A_{bpi}\gamma_{bpi}} \tag{41}$$

It is important to note, however, that the result from Eq. (41) is correct only when it is smaller than the thickness of soil, if not, it should be the thickness of soil h_{so}. The material consumption of the pile is expressed as

$$Q_{bpi} = A_{bpi}\gamma_{bpi} h_{sp} \tag{42}$$

Then, the material consumption of the bored pile is obtained by adding up the material consumption of the pile cap and the piles, as follows

$$Q_{bpb} = Q_{bp} + n_{bp} Q_{bpi} \tag{43}$$

The cost of the bored pile and the cost of the substructure adopting bored piles are expressed in Eqs. (44) and (45), respectively

$$C_{bpb} = \mu_{bp} Q_{bp} + \mu_{bpi} n_{bp} Q_{bpi} \tag{44}$$

$$C_{base} = n_{base} C_{bpb} \tag{45}$$

where μ_{bp} is the unit cost of the pile caps, μ_{bpi} is the unit cost of the bored piles, and n_{base} is the number of bridge foundations.

3.2 Concrete caissons

Fig. 9 offers the sketch of a concrete caisson. The material consumption of the concrete caisson could be calculated by referring to Eq. (32)

$$Q_{ca} = A_{cat}\sigma_{ca}\left\{\exp\left[\frac{\gamma_{ca}}{\sigma_{ca}}\left(h_w + h_{so}\right)\right] - 1\right\} - A_{cat}\gamma_{ca}\left(h_w + h_{so}\right) + N_{bs}\frac{\gamma_{ca}}{\sigma_{ca}}\left(h_w + h_{so}\right) \tag{46}$$

where Q_{ca} is the material consumption of the concrete caisson, A_{cat} is the section area on the caisson top, and N_{bs} is the compression from the tower pedestal. N_{bs} is shown in Eq. (47)

$$N_{bs} = N_{t2} + N_{tp} \tag{47}$$

where N_{t2} is the compression from the tower calculated by Eq. (19); and N_{tp} is the tower pedestal weight Q_{tp}.

The size of A_{cat} is assumed to be proportion to the section area of the pedestal according to the pile cap calculation expressed in Eq. (35), as follows

$$A_{cat} = C_{cat} A_{tpb} \tag{48}$$

where A_{tpb} is the section area on the tower pedestal bottom; C_{cat} is the ratio coefficient of the two section areas that is about equal to 2.48 referring to Great Belt East Bridge.

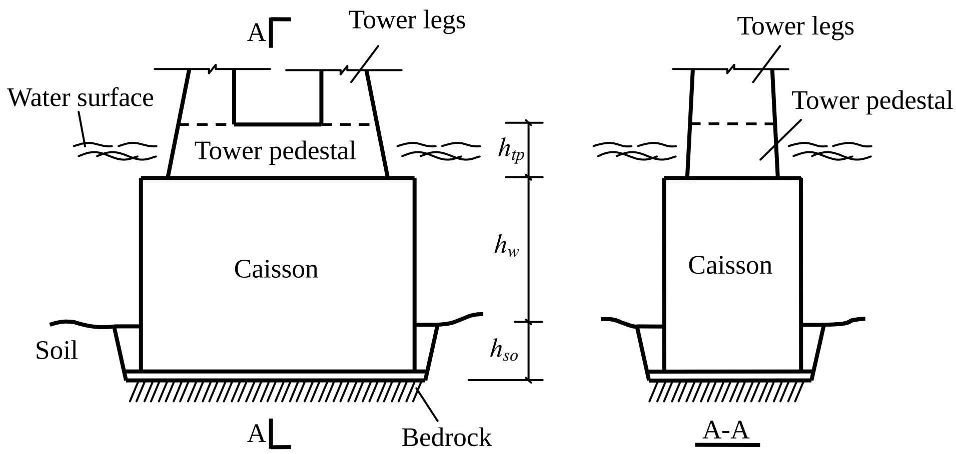

Fig. 9 Sketch of the caisson

As for the tower pedestal, it is designed mainly based on the condition of the tower bottom such as its section area and the distance between tower legs. Similarly, Great Belt East Bridge is referred for defining the section area of the pedestal. The section area is expressed as follows

$$\begin{cases} A_{tpt} = C_{tpt} A_{t2} \\ A_{tpb} = C_{tpb} A_{t2} \\ h_{tp} = C_{tph} A_{t2} \end{cases} \tag{49}$$

where A_{tpt} is the section area on the tower pedestal top; h_{tp} is the height of the tower pedestal; A_{t2} is the section area on the tower bottom; C_{tpt}, C_{tpb} and C_{tph} is the ratio coefficient of the pedestal top section area, the pedestal bottom section area and the pedestal height to the tower bottom section area, which equals 4.92, 6.332 and 0.141. The material consumption of the tower pedestal is expressed as

$$Q_{tp} = \frac{A_{tpt} + A_{tpb}}{2} h_{tp} \gamma_{tp} \tag{50}$$

N_{ca} could be obtained by substituting Eq. (50) into Eq. (47). Then, the material consumption of the concrete caisson base is expressed as follows

$$Q_{ccb} = Q_{tp} + Q_{ca} \tag{51}$$

The cost of the concrete caisson and the cost of the substructure adopting caissons are shown in Eqs. (52) and (53), respectively

$$C_{ccb} = \mu_{tp} Q_{tp} + \mu_{ca} Q_{ca} \tag{52}$$

$$C_{base} = n_{base} C_{ccb} \tag{53}$$

where μ_{tp} is the unit cost of the tower pedestal, and μ_{ca} is the unit cost of the caisson.

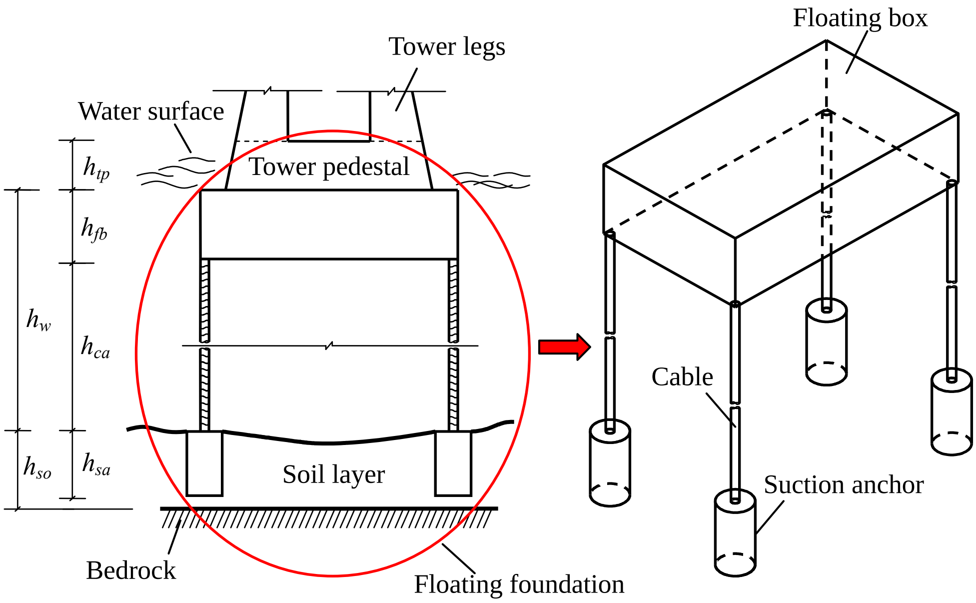

Fig. 10 Sketch of the floating foundation

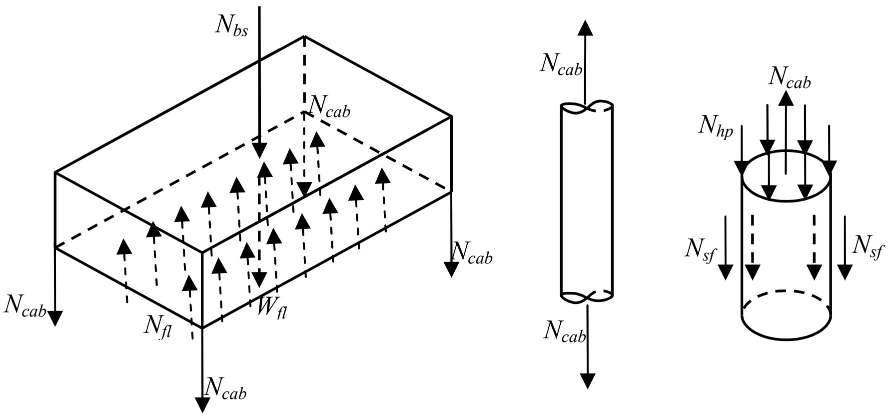

Fig. 11 Force acting on the floating box, the cable and the suction anchor

3.3 Floating foundation

The conception of floating foundations has been applied to develop the tension leg platform called "TLP" and the spar platform called "SP", which is originally proposed by Marsh in1954 and Horton in 1987 (Jiang 2010) for deeper water petroleum productions respectively. Jiang proposes a floating foundation appropriate for bridges based on TLP and SP in 2010 (Jiang 2010). The structural details of a floating foundation are shown in Fig. 10, which consists of the floating box, the cables and the suction anchors. In Fig. 10, h_{fb} is the height of the floating box; h_{ca} is the length of the cable connecting the floating box and the suction anchor; and h_{sa} is the height of the suction anchor.

In this system the force from the superstructure transfers to the floating box, being balanced by the floatage of the floating box. The floating box carries the tension of the cables between the floating box and the suction anchors. The tension of the cables is used to fix the floating box by connecting with the suction anchors, and it is balanced by the hydrostatic pressure and the soil side friction acting on the suction anchors.

Fig. 11 shows the condition of the force acting on the floating foundation, in which W_{fl} is the weight of the floating box, N_{bs} is the force from the tower, N_{cab} is the cable tension, N_{fl} is the floatage of the floating box, and N_{hp} and N_{sf} is the hydrostatic pressure and the soil side friction acting on the suction anchor respectively.

As for N_{bs}, it could be calculated by Eqs. (47) and (49). As for N_{fl} and N_{hp}, they are expressed as

$$N_{fl} = \rho_w g V_{fl} \tag{54}$$

$$N_{hp} = \rho_w g h_w A_{sa} \tag{55}$$

where ρ_w is the density of water; g is the acceleration of gravity; A_{sa} is the section area on the suction anchor top; and V_{fl} is the volume of the floating box.

The size of this system is difficulty determined not only because of its complexity, but also more because it is never designed. Thus, only the approximate calculation is carried out. An assumption that the floatage and the weight of the floating box is proportion to N_{bs} is proposed. N_{fl} and Q_{fl} is expressed as

$$\begin{cases} N_{fl} = C_{Nfl} N_{bs} \\ Q_{fl} = C_{Wfl} N_{bs} \end{cases} \tag{56}$$

where C_{Nfl} and C_{Wfl} is the ratio coefficient of the floating box floatage and weight to N_{bs} respectively. They could be obtained by referring to the study of Jiang (2010), which is 2.11 and 0.692 respectively. Eq. (57) is established based on the mechanical balance of the floating box, as follows

$$Q_{fl} + 4N_{cab} + N_{bs} = N_{fl} \tag{57}$$

Based on Eq. (57), the tension of each cable is obtained, as follows

$$N_{cab} = \frac{N_{bs}}{4}\left(C_{Nfl} - 1 - C_{Wfl}\right) \tag{58}$$

Then, the material consumption of each cable is expressed as

$$Q_{cab} = \frac{N_{cab}}{\sigma_{cab}} \gamma_{cab} h_{ca} \tag{59}$$

where Q_{cab} is the material consumption of the cable, σ_{cab} is the tension strength of the cable, and γ_{cab} is the volume-weight of the cable. As for the suction anchor, a balance equation could be established by using the same method, as follows

$$N_{cab} = N_{sf} + N_{hp} \tag{60}$$

where N_{sf} could be calculated by Eq. (40). Eq. (60) is transformed to Eq. (61) after taking Eqs. (40) and (56) in it.

$$N_{cab} = D_{sao}\pi q_{sk}h_{sa} + D_{sai}\pi q_{sk}h_{sa} + \rho_w g h_w \frac{D_{sao}^2}{4}\pi \tag{61}$$

where D_{sao} and D_{sai} is the outside diameter and inside diameter of the suction anchor, respectively.

However, it is difficult to define D_{sao}, D_{sai} and h_{as} only by Eq. (61). An assumption that the suction anchor height is proportional to its outside diameter is introduced for solving Eq. (61), as follows

$$\begin{cases} D_{sai} = D_{sao} - 2t_{sa} \\ h_{sa} = C_{sah}D_{sao} \end{cases} \tag{62}$$

where t_{sa} is the wall thickness of the suction anchor, and C_{sah} is the ratio coefficient of the suction anchor height to the outside diameter. Generally, the reasonable range of t_{sa} and C_{sah} is from 25mm to 75mm and from 4 to 12 (Jiang 2010) respectively. t_{sa} of 50mm and C_{sah} of 8 are adopted as a medium value in Eq. (62).

Additionally, D_{sai} could be recognized to equal D_{sao} for a smaller t_{sa}. Thus, h_{sa} is obtained after taking Eq. (62) into Eq. (61), which is expressed as

$$h_{sa} = \sqrt{N_{cab} \Big/ \left(2C_{sah}\pi q_{sk} + \frac{C_{sah}^2}{4}\rho_w g h_w \pi\right)} \tag{63}$$

Nevertheless, the suction anchor height calculated by Eq. (63) is acceptable only when it is smaller than the thickness of soil; if not, it equals the thickness of soil. D_{sao} then need to be obtained by solving Eq. (61) after taking the soil thickness into this equation, just as shown

$$D_{sao} = \frac{\sqrt{16\left(\pi q_{sk}h_{sa}\right)^2 + 4N_{cab}\rho_w g h_w \pi} - 4\pi q_{sk}h_{sa}}{\rho_w g h_w \pi} \tag{64}$$

D_{sai} and h_{sa} is obtained by taking t_{sa} and C_{sah} in Eq. (64). And the volume and the material consumption of the suction anchor are calculated by

$$\begin{cases} V_{sa} = \dfrac{D_{sao}^2}{4}\pi t_{sa} + \dfrac{t_{sa}\left(D_{sao} + D_{sai}\right)}{2}\pi h_{sa} \\ Q_{sa} = V_{sa}\gamma_{sa} \end{cases} \tag{65}$$

The cost of the floating foundation is expressed as follows

$$C_{flf} = \mu_{fl}Q_{fl} + 4\mu_{cab}Q_{cab} + 4\mu_{sa}Q_{sa} + \mu_{tp}Q_{tp} \tag{66}$$

where μ_{fl} is the unit cost of the floating box, μ_{cab} is the unit cost of the cables, and μ_{sa} is the unit cost of the suction anchors. And the cost of the substructure adopting floating foundations is calculated by

$$C_{base} = n_{base}C_{flf} \tag{67}$$

Table 1 Basic parameters

Parameters	Contents	Values
l_m	Main span length	1000m
l_s	Side span length	200m
f_m	Cable sag	100m
l_{rm}	Midspan suspender length	1m
h_b	Tower height above pavement	101m
h_f	Tower height below pavement	70m
h_t	Tower height	171m
g_b	Unit weight of main cable	2.65×10^5N/m
p	Live load	3.91×10^4N/m
ρ_w	Water density	1.0×10^3kg/m^3
g	Acceleration of gravity	9.8N/kg
q_{sk}	Side friction of soil stratum	40kPa
q_{sr}	Bearing capacity of soil stratum	1600kPa

Table 2 Material parameters

Parameters	Contents	Values
γ_r, γ_c	Volume-weight of suspender and main cable	85kN/m^3
γ_t	Volume-weight of bridge tower	26kN/m^3
γ_{tp}	Volume-weight of tower pedestal	26kN/m^3
σ_r	Tension strength of suspender	400MPa
σ_c	Tension strength of main cable	668MPa
σ_t	Compressive strength of bridge tower considering reduction of bending stress	13.44MPa
σ_{a1}	Compressive strength of anchorage	18.4MPa
γ_{a2}, γ_{ca}	Volume-weight of concrete caisson	26kN/m^3
γ_{bp}, γ_{bpi}	Volume-weight of pile cap and bored pile	26kN/m^3
σ_{bpi}	Compressive strength of bored pile	13.8MPa
σ_{a2}, σ_{ca}	Compressive strength of concrete caisson	13.8MPa

4. Defining of basic parameters and coefficients

4.1 Basic parameters

The basic parameters of a general suspension bridge, such as span length, sag ratio and tower height, are introduced and shown in Table 1. Additionally, all of main spans are assumed to be of equal parameters, and a soil stratum composed of the clay soil is adopted having plasticity index from 0.75 to 1.

4.2 Material parameters

Some materials are adopted according to Chinese actual condition: C30 concrete is applied to construct pile caps, concrete caissons and piles; C40 concrete is applied to construct anchorages; C50 concrete is applied to construct towers; and high strength steel wire is applied to construct main cables and suspenders. The details of the material are shown in Table 2, which are collected from the Chinese code of JTG D62-2004.

Table 3 Unit cost of materials

Unit cost	Contents	Values
μ_c	Unit cost of main cable (including the cost of suspender)	2.41764×10^4￥/t (2.41764￥/N)
μ_r	Has been included in the cost of main cable	/
μ_{sa}	Unit cost of side-span anchorage (including the base under anchorage)	1.2×10^3￥/m^3 (0.046￥/N)
μ_{ma1}	Unit cost of anchorage shared by adjacent bridge (the part above water)	7.836×10^2￥/m^3 (0.03￥/N)
μ_t	Unit cost of bridge tower	2.2202×10^3￥/m^3 (0.0853￥/N)
μ_{ma2}, μ_{ca}	Unit cost of concrete caisson	8.727×10^2￥/m^3 (0.0335￥/N)
μ_g	Unit cost of girder	1.15522×10^4￥/t (1.15522￥/N)
μ_{bp}	Unit cost of bearing platform	7.671×10^2￥/m^3 (0.0295￥/N)

Table 4 Unit cost of bored pile (μ_{bpi})

Water depth (m)	0	3	5	10	20
Cost (￥/m^3)	1154	1632.4	1835.5	2132.6	2463.7

4.3 Unit cost

It is difficult to define a universal price of the material since each country has its own specific national conditions. Thus, the material unit cost is determined mainly according to the Chinese code of JTG/T M21-2011 and some bridges in China, which are shown in Table 3.

Except for the unit cost as a constant shown in Table 3, the unit cost of piles is a changing value relevant to water depth, just as shown in Table 4.

In Table 4, only the unit cost in the region of water depth smaller than 20m is provided because that there is no a project built in water deeper than this depth for the weak stability of long piles. However, boil piles are still adopted in deeper water after lateral strengthening in order to compare with other foundations. The unit cost of piles after lateral strengthening is assumed by referring to the equation proposed by Jiang (2010).

$$U(h) = \exp\left[0.889\frac{h-100}{100}+0.711\right]U(20),\ h\geq 20\text{m} \tag{68}$$

where $U(h)$ is the unit cost of piles in the case of water depth=h, $U(20)$ is the unit cost in a water depth of 20m that is offered in Table 4.

4.4 Parameters of floating foundation

It is determined only by referring to the codes of oil drilling platforms codified by API

Table 5 Parameters about floating foundation

Parameters	Contents	Values
γ_{cab}	Volume-weight of cable in floating foundation	85kN/m^3
γ_{sa}	Volume-weight of suction anchor	78kN/m^3
σ_{cab}	Tension strength of cable in floating foundation	150MPa
μ_{fl}	Unit cost of floating box	1.2×10^4￥/t
μ_{cab}	Unit cost of cable	3.2×10^4￥/t
μ_{sa}	Unit cost of suction anchor	1.0×10^4￥/t

(American Petroleum Institute) in 1997 and 2000**,** and by referring to the trial designs by Jiang (2010) since this foundation has never been constructed. The parameters are shown in Table 5.

5. Conclusions

The cost estimation formulas of multi-span suspension bridges are derived in this study. The characteristics of the formulas are summarized as:

• The cost calculated by the formulas includes two parts: one part is the cost of superstructure; and the other part is the cost of substructure.

• Three types of the bridge foundation are considered in the substructure.

• The unit cost of the structural details, which is counted by the statistics of some projects, and other factors are considered in the formulas as a variable parameter. These could be replaced when bridge conditions are different.

Acknowledgements

Thanks to TAO Wei-jun in Guangzhou University for the data regression. This study is supported by National Natural Science Youth Foundation of China (No. 51008223), and supported by National Key Basic Research and Development Program of China (No. 2013CB036300).

References

Buckland, P.G. and Matson, D.D. (2006), "Increasing the load capacity of major bridges", *Proceeding of IABSE Symposium on Maintenance and Rehabilitation of Large Infrastructure Projects*, *Bridges and Tunnels*, Copenhagen, Denmark, January.

Clemente, P., Nicolosi, G. and Raithel, A. (2000), "Premliminary design of very long-span suspension bridges", *Eng. Struct.*, **22**, 1699-1706.

Choi, D.H., Na, H.S., Gwon, S.G., Yoo, D.H. and Moon, C. (2010), "A parametric study on the ultimate behaviors of multi-span suspension bridges", *Proceeding of 34th International Symposium on Bridge and Structural Engineering*, Venice, Italy, September.

Daniel, R.A., Dooren, F.J.V. and Meijer, R.H.D. (2010), "Comparison of a single and double main-span suspension bridge for the Western Scheldt crossing", *Proceeding of the 34th International Symposium on Bridge and Structural Engineering*, Venice, Italy, January.

Fosberp, T. (2001), "Multi-span suspension bridges", *Steel. Struct*., **1**, 63-73.

Ge, Y.J. and Xiang, H.F. (2006), “Tomorrow’s challenge in bridge span length”, *Proceedings of IABSE Symposium on Responding to Tomorrow's Challenges in Structural Engineering*, Budapest, September.
Ge, Y.J. and Xiang, H.F. (2008a), “Aerodynamic challenges in long-span bridges”, *Proceeding of IstructE Centenary Conference*, HongKong, China, January.
Ge, Y.J. and Xiang, H.F. (2008b), “Bridging capacity innovations on cable-supported bridges”, *Proceeding of the 4th International Conference on Bridge Maintenance*, *Safety and Management*, Seoul, Korea, July.
Ge, Y.J. and Xiang, H.F. (2011), “Extension of bridging capacity of cable-supported bridges using double main-spans or twin parallel decks solutions”, *Struct. Infras. Eng.*, **7**(7-8), 551-567.
Gimsing, N.J. (2012), *Cable Supported Bridges-Concept＆Design, Third Edition*, John Wiley＆Sons Ltd., Chichester.
Gimsing, N.J. (2009), “From bridges across Great Belt and Oresund towards a Femern Belt Bridge”, *Proceeding of IABSE Symposium*, Shanghai, China, January.
Hayashikawa, T. and Watanabe, N. (1982), “Suspension bridge response to moving loads”, *J. Eng. Mech. Div*., **108**(6). 1051-1066.
Jiang, H.X. (2010), “*Study on structural systems in sea-crossing bridge of floating deep-water foundation”,* Ph.D. Dissertation, Tongji University, Shanghai, China. (in Chinese)
Jung, J., Kim, J., Baek, J. and Choi. H. (2010), “Practical design of continuous two main-span suspension bridge in Korea”, *Proceeding of 34th International Symposium on Bridge and Structural Engineering*, Venice, Italy, September.
Kitagawa, M., Kashima, N., Fukunaga, S., Anzar, M.A.C.M. and Moriya, T. (2001), “Stability studies of ultra-long four span suspension bridge”, *Proceeding of IABSE Conference on Cable-supported Bridges*, Seoul, Korea, August.
Lewis, W.J. (2012), “A mathematical model for assessment of material requirements for cable supported bridges: Implication for conceptual design”, *Eng. Struct*., **42**, 266-277.
Luo, X.Y., Wang, D.L. and Chen, A.R. (2011), “The landscape design and form finding study of Taizhou Yangtze river highway bridge”, *International Conference on Electric Technology and Civil Engineering*, Wuhan, China, April.
Nazir, C.P. (1986), “Multispan balanced suspension bridge”, *J. Bridge. Eng.*, **110**(3), 392-404.
Recommended Practice for Planning (1997), *Designing and Constructing Tension Leg Platform*, American Petroleum Institute, Pennsylvania.
Recommended Practice for Planning (2000), *Designing and Constructing Fixed Offshore Platforms-Working Stress Design*, American Petroleum Institute, Pennsylvania.
Sato, K. (1971), “Deflection theory of multi-span suspension bridges considering deflection of towers and its numerical examples of various influence lines”, *Proceedings of Japan Society Civil Engineering*, Japan. (in Japanese)
Starossek, U. (1996), “Cable-stayed bridge concept for longer spans”, *J. Bridge. Eng*., **1**(3), 99-103.
Svensson, H. (2007), “The development of cable-stayed bridges since John Robling”, *Proceeding of IABSE Symposium*, Weimar, Germany, January.
Sun, B., Chen, J. and Xiao, R.C. (2010), “Preliminary design and parametric study of 1400m partially earth-anchored cable-stayed bridge”, *Sci. China Technol. Sci.*, **53**(2), 502-511.
Tang, M.C. (2007), “Evolution of bridge technology”, *Proceeding of IABSE Symposium*, Weimar, Germany, January.
Virlogeux, M. (1999), “Recent evolution of cable-stayed bridges”, *Eng. Struct*., **21**, 737-755.
Yoshida, O., Okuda, M. and Moriya, T. (2004), “Structural characteristics and applicability of four-span suspension bridge”, *J. Bridge. Eng.*, **9**(5), 453-463.
Yoshimura, T. and Kawahara, M. (2010), “Aerodynamic stability of large suspension bridge using cable frames”, *Proceeding of the 34th International Symposium on Bridge and Structural Engineering*, Venice, Italy, January.
Zhang, W.M., Ge, Y.J. and Levitan, M.L. (2011), “Aerodynamic flutter analysis of a new suspension bridge with double main spans”, *Wind Struct*., **14**(3), 187-208.

Zhang, L.W., Xiao, R.C. and Xia, R.J. (2011a), "Mechanical analysis and study on structural parameter of partially earth-anchored cable-stayed bridge part one: mechanical analysis", *Appl. Mech. Mater*., **44-47**, 1898-1905.

Zhang, L.W., Xiao, R.C. and Xia, R.J. (2011b), "Mechanical analysis and study on structural parameter of partially earth-anchored cable-stayed bridge part two: parametric study", *Appl. Mech. Mater*., **44-47**, 1906-1912.

Zhang, L.W. and Xia, R.J. (2011c), "The reasonable finished dead state research of partially earth-anchored cable-stayed bridge", *Adv. Mater. Res*., **255-260**, 1319-1325.

Zhang, L.W., Xiao, R.C., Jiang, Y. and Chai, S.B. (2012), "The characteristics of the multi-span suspension bridge with double main cables in the vertical plane", *Struct. Eng. Mech*., **42**(3), 291-311